

OFFSET AND DRIFT ANALYSIS OF THE HALL EFFECT SENSORS. THE GEOMETRICAL PARAMETERS INFLUENCE

MARIA-ALEXANDRA PAUN*, JEAN-MICHEL SALLESE, MAHER KAYAL
*STI-IEL-Electronics Lab, Ecole Polytechnique Fédérale de Lausanne (EPFL)
CH-1015 Lausanne, Switzerland*

Several Hall sensor configurations have been integrated in CMOS 0.35 μm technology and analyzed in terms of offset at room temperature and offset drift. We searched for the best geometry that would minimize the offset and its corresponding drift. The targeted specifications were $\pm 30 \mu\text{T}$ for offset at room temperature and $\pm 0.3 \mu\text{T}/^\circ\text{C}$ for the drift. The measurement setup developed to test the Hall Effect sensors allows a clean, reliable and fast analysis of a high number of the same type of cell, located on different positions on the chip. For each structure, information about the absolute sensitivity, residual offset and its drift is obtained. An important number of chips were tested in order to also provide statistical data. Maximization of the geometrical correction factor was also performed for Hall structures with small sensing contacts in order to ensure maximum sensitivity.

(Received May 4, 2012; Accepted June 20, 2012)

Keywords-Hall effect sensor, Offset, Temperature drift, Absolute sensitivity, Automated measurements

1. Introduction

The magnetic sensors are used in many applications, for example in the DC brushless motor, for the contactless measurements of mechanical quantities like position or angle. They are also used for direct magnetic field sensing, as in electronic compasses. Silicon Hall sensors are often prime candidates for such applications due to their cost-effective integration potential, reflecting in low cost, robustness and versatility [1]. CMOS technology has also the advantage of easy co-integration with electronics on the same chip. The Hall Effect is based on magnetic field influence acting perpendicularly on a semiconducting structure carrying a certain electric current. Because on the moving charge carriers in a magnetic field acts the Lorentz force, a new voltage arises. This voltage named Hall voltage is recorded perpendicular to the direction of current flow. New research is devoted to submicron Hall Effect sensors which are nowadays used for the detection of the supermagnetic beads [2].

As it is known, the principal accuracy limitations that affect Hall Effect sensors performances are the offset and its temperature drift [3]. Some of the generation causes for offset are related to the fabrication process of a Hall cell, packaging, operating conditions and ageing [4]. The major source for the offset voltages apparition is the imbalances of the Hall plate. Therefore, a real Hall sensor could have a zero-field offset due to possible geometrical mismatches. In order to eliminate the offset of Hall sensors, the dynamic method known as “current-spinning technique” is used [5]. An important figure of merit of these sensors is the sensitivity which is strongly limited by the short-circuit effects. A high absolute sensitivity improves the signal-to-noise ratio of magnetic sensors [6].

The present paper aims at developing several Hall sensor geometries to fit in targeted offset and drift specifications, then analyze the offset and drift of these structures by using a reliable, automated measurement setup and finally identify the geometry that would best minimize

* Corresponding author: maria-alexandra.paun@epfl.ch

these quantities of interest. As the geometrical correction factor is linked to sensitivity, this figure of merit was analyzed and maximized for certain geometries with small contacts.

2. Hall effect sensors integration

2.1. Hall Effect sensors sensitivity and offset

Sensitivity is one of the most important figures of merit related to a sensor. In general, the sensitivity is defined as the change in output resulting from a given change in input. Consequently, both absolute and relative sensitivities can be introduced. The absolute sensitivity of a Hall magnetic sensor is considered as given by the equation below

$$S_A = \left| \frac{V_{HALL}}{B_{\perp}} \right| \quad (1)$$

where V_{HALL} is the Hall voltage and B_{\perp} is the normal component of the magnetic induction [7]. In order to have a maximum sensitivity, for a given fabrication process, we could proceed to maximize the geometrical correction factor, G , as was analyzed by the authors in a recent paper [8]. This can give an idea on how to actually choose the dimensions and contacts of the Hall cells such that to achieve the maximum sensitivity.

The offset is an undesired parasitic voltage that adds to the Hall voltage. Therefore, the total voltage is

$$V_{total} = V_{offset} + V_{HALL}(B) \quad (2)$$

where V_{offset} is the offset voltage in the absence of the magnetic field, V_{HALL} is the Hall voltage and B is the magnetic field induction.

For the magnetic sensors, it is also important to analyze the magnetic field equivalent residual offset (two or four-phase current spinning can be employed) of the Hall device, in Tesla, which is given by the following relationship

$$B_{offset}^{residual} = \frac{V_{offset, residual}}{S_A} \quad (3)$$

where $V_{offset, residual}$ in Volts is the residual offset voltage, obtained after the application of the current spinning technique and S_A is the absolute sensitivity, in V/T.

2.2. Hall cells configurations

The geometry has a great importance in the Hall Effect sensors performance. The first qualitative reasoning premise for choosing the 4 Hall cell structures consists in fulfilling the symmetry and invariance to $\pi/2$ for further good application of the current-spinning technique for reducing the residual offset. The cells are integrated in an XFAB 0.35 μm Si CMOS technology and designed in CADENCE. Different geometries were proposed like the regular Greek cross and three other variations (45 Deg, XL, Narrow contacts).

The basic cell was implemented as a reference, but it might suffer from a difference in the piezo-resistance due to the orientation of the cross. Therefore, the 45 degrees cell was also integrated. The mechanical stress will less affect the piezo-resistance in this case, due to the orientation of the current density with respect to the Si crystallographic axes [9]. The increase of the cell dimensions led to XL cell implementation. This configuration was chosen in order to minimize the errors of the contour which become less important in this case, due to their averaging on a greater size. This assumption is confirmed experimentally as well. The narrow contacts cell prevents shunting of the current and by having small sensing contacts it improves the sensitivity.

Compact models of cross-shaped Hall sensors have recently been developed [10]. The performances of horizontal Hall sensors in CMOS technology greatly improved over the last years. Hall devices with offset less than 10 μV [11] and integrated Hall sensors with an offset drift lower than 1.5 $\mu\text{T}/^\circ\text{C}$ [12] were reported.



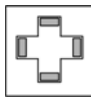
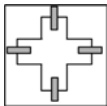
The four analyzed geometries, in ascending order of their measured internal resistance, together with their specific parameters are presented in Table 1. W , L , s stand for Hall cells width, length and sensing contact length respectively. The geometrical correction factor, G , models the reduction of V_H due to the part of the current which flows through the sensing contacts. This figure of merit was computed for each geometry, using the equation presented in [7].

$$G \cong 1 - \frac{16}{\pi^2} \exp\left(-\frac{\pi L}{2W}\right) \left[1 - \frac{8}{9} \exp\left(-\frac{\pi L}{2W}\right)\right] \left(1 - \frac{\theta_H^2}{3}\right) \quad (4)$$

valid if $0.85 \leq L/W < \infty$ and $0 \leq \theta_H \leq 0.45$.

The offset drift value is averaged on all the tested samples.

Table 1. Hall cell geometries design parameters

Type of Hall cell	45 Deg	XL	Basic	Narrow contact s
Geometry				
L(μm)	21.6	43.2	21.6	21.6
W(μm)	11.8	22.6	11.8	9.5
R(k Ω)	2.1	2.2	2.3	2.5
G	0.913	0.924	0.913	0.870
s(μm)	11	20.7	11	1.5
S _A (V/T) I=1mA	0.082	0.082	0.082	0.088
Average offset drift ($\mu\text{T}/^\circ\text{C}$)	0.373	0.039	0.409	0.344

3. Geometrical correction factor analysis

Narrow contacts cell behaves well in terms of offset and offset drift and has the highest sensitivity, as validated by the authors in a recent paper for geometries with small contacts [8]. This type of geometry led to further investigations for small contacts geometries and their sensitivity improvement.

Therefore we maximize the geometrical correction factor to ensure the maximum sensitivity. We perform this analysis for cells manufactured with the same fabrication process. In this situation, for structures with small sensing contacts of dimension s , and imposed area A , the geometrical correction factor rewrites as:

$$G = \left(1 - e^{-\frac{\pi A}{2W^2}}\right) \left(1 - \frac{2s}{\pi W}\right) \quad (5)$$

valid for $A/W^2 > 1.5$ and $s/W < 0.18$.

The 3D figure below was simulated in MATLAB. Therefore, Fig. 1 depicts the three-dimensional representation of the geometrical correction factor as function of sensors width and area. W varies from 10 to 60 μm , A from 100 to 3600 μm^2 and three different values for s (0.5, 1 and 1.5 μm) were employed. We can clearly see the zone where the indicator G is maximum, this occurring for the largest area and smallest width, equivalent to the largest L/W . The smaller the contacts, the higher the geometrical correction factor, as G increases with the decrease of s/W , for the same W and A .

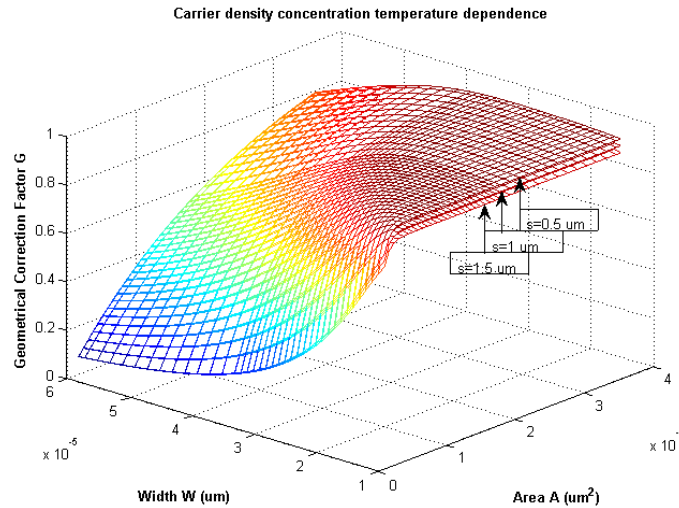


Fig. 1.3D representation of the geometrical correction factor as function of width W and area A

Fig. 2 shows how the designer should choose the best Hall cell design, in terms of length-to-width ratio, for maximum sensitivity, when disposing of a certain available Si area, A , and specific small sensing contacts, s .

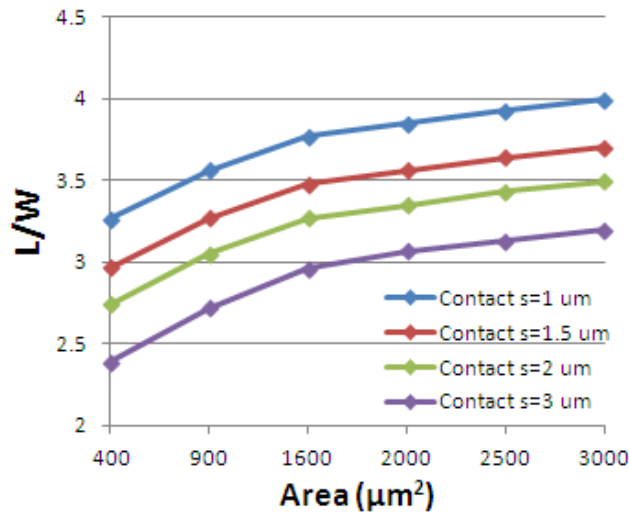


Fig. 2. Variation of L/W with respect to area A , for different small sensing contact sizes, s

4. Measurement setup

For testing the proposed geometries we developed an automated AC measurement procedure. While DC measurements might have more noise, the AC is more accurate especially at lower frequencies. An advantage of automated measurements is that all the cells can be tested under the same conditions, also allowing averaging on a large number of acquisitions. This system is reliable, fast and the samples are very well protected.

A Digital Acquisition Card (DAQ) from National Instruments and LABVIEW programs were used for the address control and collecting results respectively. To test 8 times the 4 cells, we used a multiplexer MUX 4X8 and digital representation (by addresses) for selecting the cells. Hall cells were biased between 0 and 1 mA, using a Keithley K220 current source, with a compliance voltage set at 5 V.

The frequency used for measurements was 37 Hz, while the reference frequency $root_f$ used for the demodulation was half. A switching circuit rotates the bias current source and sensor output voltage terminals between pairs of orthogonal contacts, to differentiate between the 4 phases.

For read out, the offset was collected with a lock-in amplifier, which provided us directly the averaged offset, after the application of the 4-phases current spinning technique over a time period. An amplifier with a gain of 100 was used for offset read-out. In this way we can easily extract residual offset and decide which cell is the best in terms of minimum residual offset. The automated AC measurement setup is presented in Fig. 3.

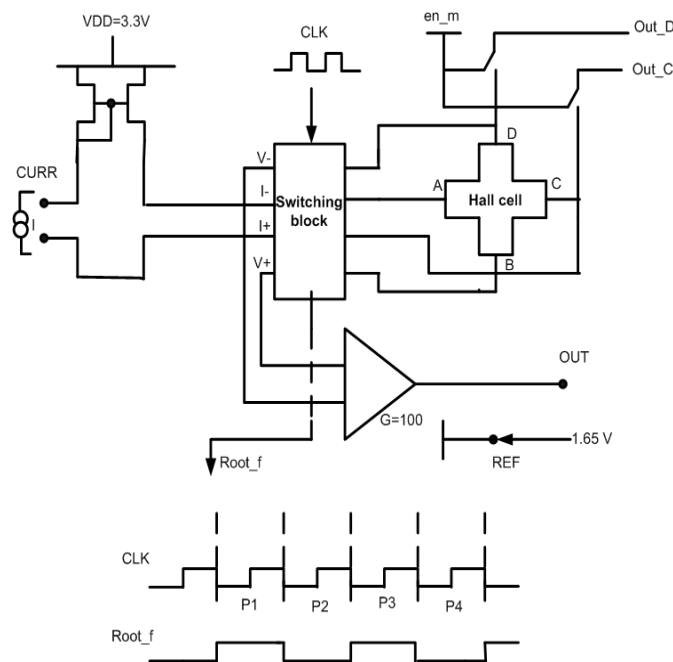


Fig. 3. The automated AC measurement setup

The same setup could be transformed to suit DC measurements. In this case we enable all the switches, to have access to punctual output voltage information, in this way being able to discriminate between the different phases.

On the DAQ in addition to the already used digital input outputs (DIO), some analog inputs and outputs will be used. Analog Output (AO) will be coupled to the reset and Analog Input (AI) will be used for the $root_f$. Along with the addresses, in DC, the clock will be used as a digital input. All the measurement units and the Hall Cell Chip are connected to the same ground point. The instruments setup is presented in Fig. 4.

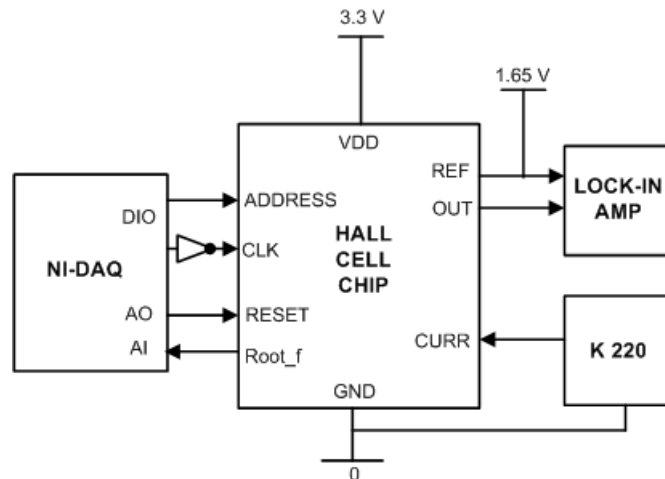


Fig. 4. The main blocks of the measurement setup

5. Results and discussion

We investigated the room temperature offset and its drift behavior for several Hall cell configurations in order to find the best geometry that would minimize these quantities. In this sense 11 samples, each one containing 32 cells, were tested. The positioning of the four cells as repetition of eight is presented in Figure 5. We took care to have the same cell several times and at different locations on the chip in order to face representation of possible variations. The experimental results were both statistically processed and interpreted. The values obtained are in accordance with the state-of-the-art.

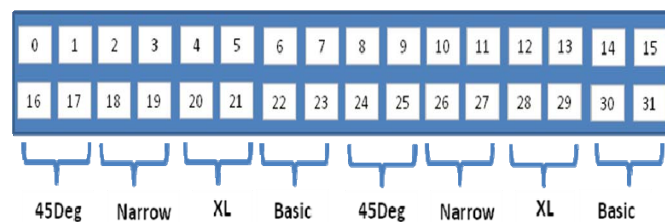


Fig. 6. Positioning of cells onto the tested chip

The temperature measurements for offset drift were performed using a TEMPTRONIC oven in a range considered from $-25\text{ }^{\circ}\text{C}$ to $95\text{ }^{\circ}\text{C}$. The average offset drift ($\mu\text{T}/^{\circ}\text{C}$) was 0.409 for basic cell, 0.373 for 45 Deg, 0.039 for XL and 0.344 for narrow contacts. All the configurations approached very close the targeted specifications of $\pm 0.3\text{ }\mu\text{T}/^{\circ}\text{C}$, but XL cell distinguishes with the lowest offset drift, almost ten times lower than for the other configurations. The offset drift average standard deviation ($\mu\text{T}/^{\circ}\text{C}$) for all 11 tested samples was 0.02 for XL, 0.03 for narrow contacts cell and 0.05 for basic and 45 Deg cells respectively.

We were interested in the variation of the magnetic field equivalent residual offset as a function of the biasing current, for the proposed geometries. When computing the magnetic field equivalent residual offset, the curves used for the sensitivity (V/T) for each cell were obtained under a constant magnetic field, generated by a NMR permanent magnet of magnetic induction $B=0.497\text{ T}$, perpendicular to the probe. The absolute sensitivity is presented for all the cells in the following table, for certain important biasing currents.

Table 2. Hall cells absolute sensitivity (v/t)

I_{bias} (mA)	45 Deg	XL	Basic	Narrow c.
0.20	0.0158	0.0157	0.0159	0.0165
0.30	0.0241	0.0240	0.0242	0.0252
0.50	0.0414	0.0412	0.0416	0.0433
0.80	0.0627	0.0628	0.0626	0.0628
0.85	0.0630	0.0630	0.0630	0.0630

Fig. 6 - Fig. 9 display the magnetic field equivalent residual offset characteristics at room temperature with respect to the biasing current, for all the proposed cells, where each geometry is replicated and measured 8 times on the chip, at different positions. The light blue band represents the specifications set for room temperature offset, which correspond to values less than $30 \mu\text{T}$. The experimental data is processed and presented for biasing currents of interest up to 0.85 mA which correspond to an absolute sensitivity of 0.063 V/T.

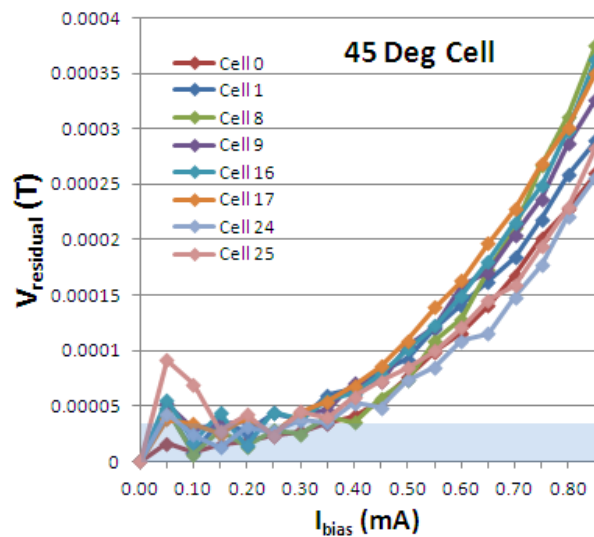


Fig. 7. Room temperature residual offset (T) for 45 Deg cell

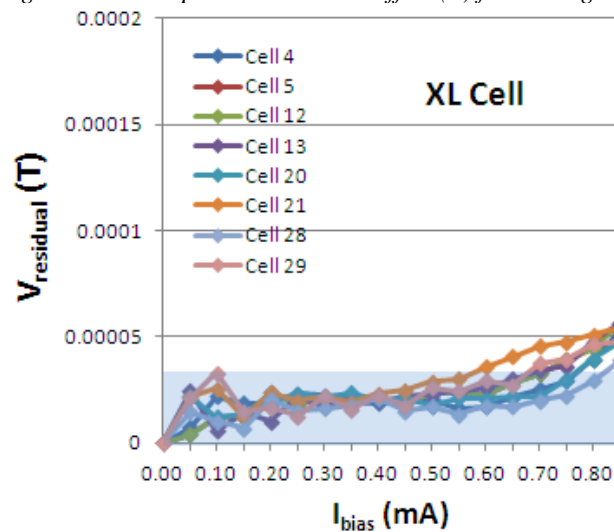


Fig. 8. Room temperature residual offset (T) for XL cell

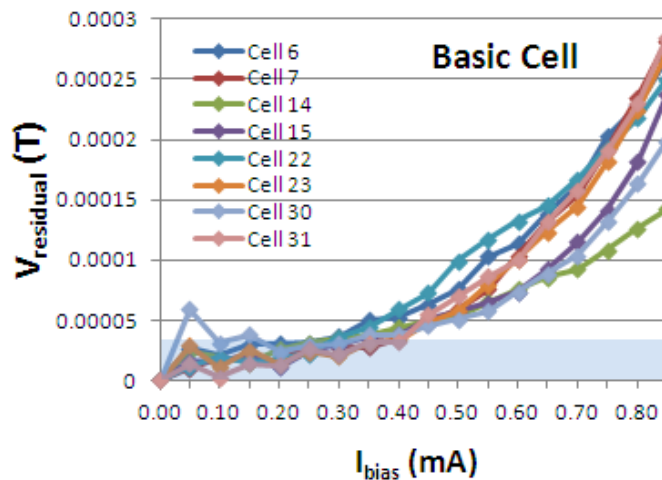


Fig. 9. Room temperature residual offset (T) for basic cell

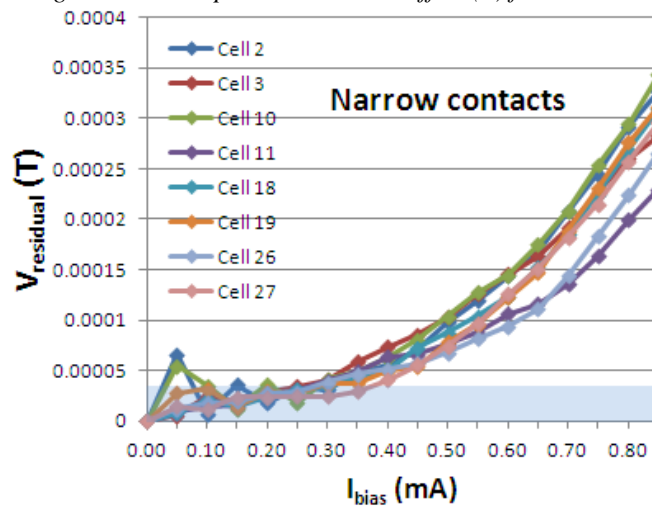


Fig. 10. Room temperature residual offset (T) for narrow contacts cell

We can observe from the previous graphs, that while the residual offset of the majority of cells is within the specification band at low biasing currents, for example a current value in the region of 0.3 mA, the XL cell fits in the proposed interval for all the values of the biasing current. A biasing current of 0.3 mA is equivalent to an absolute sensitivity of approximately 0.025 V/T.

Three-dimensional physical simulations were developed by the authors in [13] in order to estimate the offset and compare the numerical with the experimental results. This method will be used as a complementary tool for future Hall Effect sensors design.

6. Conclusions

To achieve Hall sensors geometry optimization and comparative study of the characteristic design elements, we developed adequate analysis instruments and measurement setups to estimate the offset and its drift.

We searched for the best Hall geometry that would minimize the parameters of interest. The analysis of the four proposed Hall Effect sensors, in terms of room temperature offset and offset drift was achieved using an automated measurement system, providing a fast and reliable method for offset investigation. The large number of tested samples and the possibility of evaluating multiple times each proposed Hall sensor geometry increased the measurements reliability.

The analysis performed on the set of four configurations for the Hall Cell led to good results for the room temperature offset and offset temperature drift, within the targeted specifications, and suggested the best configuration to be XL cell. For low biasing current and an

absolute sensitivity up to 0.025 V/T, all the analyzed cells satisfy the targeted offset interval, but the XL clearly distinguishes itself by fitting in this interval for almost all biasing current range of interest.

Maximization of the geometrical correction factor was also performed for Hall structures with small sensing contacts in order to ensure maximum sensitivity. In this sense, information on L/W was provided for certain available Si area and small sensing contacts. This analysis could guide the designers in choosing the optimum dimensions for the Hall cell.

Acknowledgment

This work has been supported by Swiss Innovation Promotion Agency CTI (Project 9591.1) and the company LEM SA – Geneva, Switzerland.

References

- [1] C. Muller-Schwanneke, F. Jost, K. Marx, S. Lindenkreuz, K. von Klitzing, *Sensor and Actuators A* **81**, 18 (2000).
- [2] A. Manzin, V. Nabaei, and O. Kazakova, *Journal of Applied Physics* , **111**, 07E513 - 07E513-3 (2012).
- [3] Ch. S. Roumenin, S.V. Lozanova, *Sensors and Actuators A* **138**, 37-43 (2007).
- [4] D. Manic, P. M. Igit, Y. Haddab, R. S. Popovic, *IEEE Transactions on Electron Devices*, **47**(12), (2000).
- [5] A. Kerlain, V. Mosser, *Sensor and Actuators A* **142**, 528-532 (2008).
- [6] J.-B. Kammerer, L. Hebrard, V. Frick, P. Poure, F. Braun, *IEEE Sensors Journal*, **3**(6), 700-707 (2003).
- [7] R. S. Popovic, *Hall Effect Devices*, Second Edition, Institute of Physics Publishing, 2004.
- [8] M.-A. Paun, J.-M. Sallese, M. Kayal, *U.P.B. Sci. Bull., Series A*, **72**(4), 257-271 (2010).
- [9] S. Fischer, J. Wilde, *IEEE Transactions On Advanced Packaging*, **31**(3), (2008).
- [10] M. Madec, J.-B. Kammerer, and L. Hebrard, *NEWCAS 2010 Proceedings*, *IEEE Explorer*, pp. 397-400, 2010.
- [11] Y. Hu, W.-R. Yang, “CMOS Hall Sensor Using Dynamic Quadrature Offset Cancellation”, *ICSICT 2006*, *IEEE Explorer*.
- [12] M. Pastre, M. Kayal, H. Blanchard, *IEEE Sensors Journal*, **7**(5), 860-867 (2007).
- [13] M.A. Paun, J.M. Sallese, M. Kayal, *Mixed Design of Integrated Circuits and Systems (MIXDES)*, 2011 Proceedings of the 18th International Conference , 2011 , pp. 450 – 45.